

Insight into the Catalysis of Hydrolysis of Four Newly Synthesized Substrates by Papain: A Proton Inventory Study

Leonidas G. Theodorou,[‡] Kostas Lymperopoulos[‡], Joseph G. Bieth,[§] and Emmanuel M. Papamichael^{*‡}

University of Ioannina, Department of Chemistry, Laboratory of Biochemistry, 451-10 Ioannina, Greece and
 Université Louis Pasteur Strasbourg, Faculté de Pharmacie, I.N.S.E.R.M. Unité de Recherche 392,
 Lab. d'Enzymologie, 74 Route du Rhin, Illkirch, F-67400, France

Received July 12, 2000; Revised Manuscript Received January 9, 2001

ABSTRACT: We synthesized the following four new peptide substrates, Suc-Phe-Leu-pNA, Suc-Phe-Leu-NMec, Suc-Phe-Leu-ONPh, and Pht-Phe-Leu-pNA, and we applied the proton inventory method to their hydrolysis by papain. Useful relationships between the rate constants of the catalytic reaction have been established and contributed to the elucidation of the hydrolytic mechanism of papain. For all amide substrates, the parameter K_S and the rate constants k_1 , k_{-1} , and k_2 were estimated. Moreover, it was found that $k_{cat}/K_m = k_1$ for all four substrates, while two exchangeable hydrogenic sites, one in the ground state and another in the transition state, generate an inverse isotope effect during the reaction governed by this parameter. The proton inventories of both k_2 and k_3 are essentially linear, whatever the acyl moiety and/or the leaving group of the substrate. The proton inventories of K_S are also essentially linear for all amide substrates, while the observed large isotope effect of about 3 to 9 originates from a single hydrogenic site in the product state. This latter, in agreement to both the small transition state fractionation factors found for k_{cat}/K_m (or k_1) and the unit ground-state fractionation factors found for k_2 , argues for the formation of a tetrahedral adduct during the reaction governed by the k_1 parameter. Furthermore, papain acts as a one-proton catalyst during acylation or deacylation, both of which proceed through similar concerted reaction pathways, where a nucleophilic attack is accompanied by the movement of one proton.

The proton inventory (PI)¹ method comprises kinetic studies of solvent isotope effects (SIE) in a series of mixtures of H₂O and D₂O (*I*). In this method, the reaction parameters are expressed as $k_n(n)$ functions of deuterium atom fraction n present in the isotopic solvent, according to eq 1 (2), where k_0 is the reaction parameter in H₂O.

$$k_n = k_0 \frac{\prod_{i=1}^{\mu} (1 - n + n\phi_i^T)}{\prod_{j=1}^{\nu} (1 - n + n\phi_j^G)} \quad (1)$$

In eq 1, ϕ_i^T and ϕ_j^G are the isotopic fractionation factors of *i*th transition state proton and *j*th ground-state proton, respectively. These parameters reveal the effect of solvent in the process from a reactant state to a transition state. In

addition, the shape of the $k_n(n)$ functions, the magnitude of SIE, and the number of the transferred protons are diagnostic of the reaction mechanism (*I*, 3). Tools such as SIE and PI have been widely used as probes of the mechanism of action of serine proteinases; however, they found a limited use in the family of cysteine proteinases (2, 4, 5).

Papain is a widely studied cysteine proteinase, and it is considered as a model among these enzymes (6). Its catalytic mechanism has been studied to some extent (7, 8) and is represented by the minimal Scheme 1 (9).

The side chains of residues Cys-25 and His-159 of papain form an ion-pair (Cys-25)-S⁻/(His-159)-Im⁺H (C⁻H⁺), while the substrate binds to enzyme, favored by an "oxyanion hole" (6, 10–12). Furthermore, the nucleophilic ionized active Cys-25 attacks the carbonyl carbon of the scissile amide or ester bond (12) and by releasing an amine or an alcohol a covalent acyl enzyme intermediate is formed; next, the acyl-enzyme deacylates, following a nucleophilic attack by a water molecule. Both acylation and deacylation proceed through tetrahedral intermediates, whose formation is triggered by a nucleophilic attack concerted with a proton transfer (10, 12). Although the overall catalytic process is well documented, the catalytic mechanism is poorly defined in details. Also, the relationship between the molecular structure of papain or its substrates and the catalytic reaction are not clearly understood (12).

We have synthesized four new substrates and applied the proton inventory method to their hydrolysis to investigate

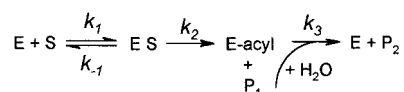
* Corresponding author: Emmanuel M. Papamichael, University of Ioannina, Department of Chemistry, Lab. of Biochemistry, 451-10 Ioannina, Greece, TEL.: +30 651 98395, FAX: +30 651 47832, E-mail: epapamic@cc.uoi.gr.

[‡] University of Ioannina.

[§] Université Louis Pasteur Strasbourg.

¹ Abbreviations: Suc, succinyl; Pht, phthalyl; pNA, *p*-nitroanilide; ONPh, *p*-nitrophenyl; NMec, 7-amino-4-methylcoumaryl; PI, proton inventory and/or inventories; SIE, solvent isotope effect; DMSO, dimethyl sulfoxide; HAR, heavy atom reorganization; PT, proton transfer; E-64, 1-[[[N-(L-3-*trans*-carboxyoxiran-2-carbonyl)-L-leucyl]-amino]-4-guanidinobutane; C⁻H⁺, (Cys-25)-S⁻/(His-159)-Im⁺H.

Scheme 1



the minimum mechanism (Scheme 1). According to our results, the ES complex has the form of a tetrahedral adduct, and it is produced during the reaction governed by the k_{cat}/K_m (or k_1) parameter where two exchangeable hydrogenic sites one in the ground state and another in the transition state generate an inverse isotope effect. Furthermore, a nucleophilic attack is concerted with proton transfer to the effective transition states, during acylation and/or deacylation processes.

EXPERIMENTAL PROCEDURES

Materials. All chemicals, including D₂O (99.9%, pD 7.4), were of analytical grade, purchased from Sigma. Twice-crystallized papain (Sigma, EC 3.4.22.2) was further purified by affinity column as described previously (13), was migrated as a single band of $M_r = 25\,000$ on SDS/PAGE electrophoresis, and was found to be more than 75% active as titrated with E-64 (14).

Methods. (a) *Synthesis.* All four substrates have the general formula Y-Phe-Leu-X, where Y = {Suc-, Pht-} and X = {pNA, ONPh, NMec}. The commonly used Arg at P₁ position was replaced by Leu having a relatively long aliphatic side chain; we considered also that an active ester of the formula Suc-X-Arg-ONPh is hardly synthesized and it would be quite unstable, due to reactivity of the side chain of Arg. All substrates were synthesized from t-BOC-Phe, CBZ-Leu and the appropriate chromophore. The Suc- and Pht- groups were incorporated as described previously (15). The phosphoazo method (16) and/or the mixed anhydride method (17), in case of the ester substrate, have been applied for the coupling of chromophores to Leu. All substrates were purified by reversed phase HPLC (Sephasil Peptide Pharmacia C₁₈), their purity was checked in TLC, and their structures were assigned by ¹H NMR spectrometry (Bruker AMX-400 MHz).

(b) *Solutions.* Phosphate buffer solutions for the PI studies allowing different values of deuterium atom fraction n in the solvent were prepared gravimetrically by mixing appropriate quantities of phosphate buffers made up in H₂O and D₂O at pL 6.5, as described previously (1, 2). All pD values were estimated using the relation pD = pH meter reading + 0.4 (1). The pH and/or pD value of the stock phosphate buffers was checked on a radiometer pH meter model PHM 82. Active site titrations were performed in phosphate buffer made up in H₂O at pH 6.5. Stock and working solutions of all the four substrates were prepared in DMSO.

(c) *Kinetic Procedures.* Initial velocities of enzymatic reactions were measured either spectrophotometrically, at 410 nm ($\epsilon_{pNA} = 8800\text{ M}^{-1}\text{ cm}^{-1}$) or at 347.5 nm ($\epsilon_{pNPh} = 5500\text{ M}^{-1}\text{ cm}^{-1}$) (18) for pNA and ONPh substrates, respectively, or spectrofluorometrically for the NMec substrate ($\lambda_{ex} = 365\text{ nm}$, $\lambda_{em} = 400\text{ nm}$). Velocities were measured with a Perkin-Elmer L15 double beam spectrophotometer, and a SPEX filter-fluorimeter connected to a recorder calibrated with standard solutions of NMec. In a typical kinetic run, the enzyme solution was diluted into the appropriate quantity

of buffer contained in a glass cuvette of 1-cm path length so that the active concentration of papain was 170 nM; then, the mixture was thermostated at 25 °C for 5 min. The reaction was initiated by addition of 10 to 50 μL of appropriate substrate solution, so that their concentrations were varied from 50 to 2000 μM , and the release of the leaving group was recorded. Self-hydrolysis of Suc-Phe-Leu-ONPh was being determined by substituting the enzyme solution by buffer solution (2), per n value and substrate concentration. Eleven different values of n ranging from 0 to 0.99 were used for each substrate and eight substrate concentrations were used, per n value, to measure the kinetic parameters (k_{cat}) _{n} and (K_m) _{n} , each single kinetic measurement being repeated eight times. The total content of DMSO was always 5% (v/v).

Additional burst kinetics of Pht-Phe-Leu-pNA hydrolysis was also performed to measure (k_2) _{n} and (k_3) _{n} separately for this substrate. We used 11 different values of n , each measurement being repeated eight times. Papain (final concentrated 8 μM) was diluted as it is mentioned above, and the spectrophotometer was set to zero absorbance. The reaction was initiated at time zero, by addition of 20 μL of substrate solution (final concentrated 520 μM). After 40 s, the progress of each reaction was followed up to a sufficient portion of the steady-state phase. In all cases, the absorbances were corrected by subtracting the absorbance of a substrate blank solution. The total content of DMSO was always 5% (v/v).

The initial velocities measurements allowed k_{cat} to be calculated while the steady-state portion of the burst progress curve (>5 min) was treated as described previously (19). By rearranging the corresponding equations of ref 19 to $B = (k_{cat}[E]/k_3)/[1 + K_m/[S]]^2$ (Appendix 1), we solved for k_3 as the positive square root value. By using the definition $k_{cat} = k_2k_3/(k_2 + k_3)$, we calculated the k_2 , and from the definition of $K_m = k_3K_s/(k_2 + k_3)$ we calculated the K_s (9).

(d) *Analysis of Data.* All (k_{cat}) _{n} and/or (K_m) _{n} parameters of this study were estimated from initial rates of hydrolysis of the substrates by nonlinear curve fitting (20) to Michaelis-Menten equation. To determine the PI, which is to determine the significance of the parameters of eq 1, we used previous theoretical approaches (1, 2). Several equations were fitted by nonlinear regression to each of the sets of experimental data (21). Equation 2 describes a general case where several exchangeable hydrogenic sites have identical fractionation factors in the ground state and/or in the transition state. Similarly, in eq 3 one site has nonunit fractionation factors in both the ground state and the transition state. Furthermore, eq 3a is used in cases of PI for equilibrium constants, where transition state has been changed to product state. Equations 4, 4a, and 4b describe cases in which up to two exchangeable hydrogenic sites have nonidentical fractionation factors in the ground state and/or in the transition state. Finally, eq 5 could be used to fit linear proton inventories.

$$k_n = k_0 \frac{(1 - n + n\phi^T)^\mu}{(1 - n + n\phi^G)^\nu} \quad (2)$$

$$k_n = k_0 \frac{1 - n + n\phi^T}{1 - n + n\phi^G} \quad (3)$$

$$K_n = K_0 \frac{1 - n + n\phi^P}{1 - n + n\phi^G} \quad (3a)$$

$$k_n = k_0 \frac{(1 - n + n\phi_1^T)(1 - n + n\phi_2^T)}{(1 - n + n\phi_1^G)(1 - n + n\phi_2^G)} \quad (4)$$

$$k_n = k_0 \frac{1 - n + n\phi^T}{(1 - n + n\phi_1^G)(1 - n + n\phi_2^G)} \quad (4a)$$

$$k_n = k_0 \frac{(1 - n + n\phi_1^T)(1 - n + n\phi_2^T)}{1 - n + n\phi^G} \quad (4b)$$

$$k_n = k_0(1 - n + n\phi^T) \quad (5)$$

To find out which equation best fitted each series of experimental data, we proceeded as follows: First, we used an unweighted nonlinear curve fitting for each series of experimental data and for each equation (20, 22). To this end, we used the least squares $[\sum_{i=1}^n w_i(y_i - \hat{y}_i)^2]$ criterion of convergence. After having established good initial parameter guessing and proper weighting factors (20–22), we performed weighted nonlinear curve fitting. Robust weighting also has been applied to delete data points whose errors are exceeding the error range of other data. We then decided that the nonlinear equations that best fitted the experimental data must fulfill the following four requirements: (a) the analysis of residuals (21, 22), (b) the Chi-square test – 95% confidence (21), (c) the F-test – 95% confidence (21), and (d) the Akaike's information criterion (AIC) (23).

On the basis of previously published results (2, 24), we considered that deacylation of acyl-papain is the overall rate-determining step for the hydrolysis of Suc-Phe-Leu-ONPh. Thereupon we introduced an approximation $k_{cat} \approx k_3$ for this substrate, and hence we assumed that $k_3(\text{Suc-Phe-Leu-ONPh}) = k_3(\text{Suc-Phe-Leu-pNA}) = k_3(\text{Suc-Phe-Leu-NMec})$ since these substrates have the same acyl enzyme intermediate. Accordingly, we calculated all $(k_2)_n$ values for the Suc-Phe-Leu-pNA and Suc-Phe-Leu-NMec substrates from relation $k_2 = k_{cat} k_3/(k_3 - k_{cat})$. By taking into account the known values of $(K_m)_n$, $(k_2)_n$, and $(k_3)_n$ parameters for all three amide substrates, we calculated their $(K_S)_n$ values using the relation $K_m = k_3 K_S/(k_2 + k_3)$ (9). A formal definition of $K_S = (k_{-1} + k_2)/k_1$ results from the steady-state treatment of the minimal mechanism of Scheme 1, and it has been suggested by others in cases where the magnitudes of k_{-1} and k_2 are comparable (19, 25). In not uncommon cases, where $k_{-1} \ll k_2$ or vice versa, K_S has a completely different meaning (25). To obtain eq 6, we assumed that all meanings of K_S are valid equally likely, and that $\phi^{T,k1} = \phi^{T,k-1}$, and $\phi^{G,k2} = \phi^{G,k-1}$. Furthermore, we substituted the rate constants of the relation $k_2/(k_{cat}/K_m) = K_S = (k_{-1} + k_2)/k_1$ according to eq 3 (Appendix 2). In eq 6, $K_R = k_2/k_1$, and $C_1 = \phi^{G,k2}$, $C_2 = \phi^{T,k2}$ and k_2 are known and have been determined (see Results, under PI of k_{cat}/K_m and/or k_2).

$$\frac{(k_2)_n}{(k_{cat}/K_m)_n} = \frac{1 - n + n\phi^{G,k1}}{1 - n + nC_1} \left[\frac{k_2}{(k_{cat}/K_m)} + K_R \left(\frac{1 - n + nC_2}{1 - n + n\phi^{T,k1}} - 1 \right) \right] \quad (6)$$

RESULTS

Proton Inventories of k_{cat}/K_m . Equation 3 best fitted the experimental data for k_{cat}/K_m as function of deuterium atom fraction n . These proton inventories exhibited high inverse SIE (5, 26) and “bowed-downward” shapes. The mean values 0.42 and 0.17 were calculated for the fractionation factors ϕ^T and ϕ^G . These results are reported in Figure 1 and in Table 1. Deviations from nonlinear fitting of individual experimental points due to the introduction of small errors in the measurements of initial velocities and/or the estimation of deuterium atom fraction present in the isotopic solvent (2) were taken into account by the robust weighting requirements. Accordingly, three experimental points corresponding to n values 0.6, 0.7, and 0.8 were eliminated from Figure 1, panel d; they contained large errors due, more likely, to calculation of $(k_{cat}/K_m)_n$ as ratios of the corresponding values of $(k_{cat})_n$ and $(K_m)_n$. Hence, we performed complementary PI experiments for the ester substrate under $[S] = (0.01, 0.02)K_m$, and from first-order progress curves we estimated directly the $(k_{cat}/K_m)_n$ values (27); these data entirely confirmed the previous ones (Figure 1, panel d, insert).

We got almost the same results, using alternative treatments of the same experimental data. We proceeded to perform: (a) a suitable reparametrization of the nonlinear equations 3 and 4 to 4c, until they became linear in their parameters (28) and (b) nonparametric curve fitting methods (21), and in most cases, we approached global minima. However, in few cases, we were supported by fair initial parameter guessing values, which were applied to the fitting of corresponding nonlinear forms. Additionally, in these procedures we applied two more diagnostic tests specific for linear equations, the variance inflation factor and the principal component analysis (28, 29), through which we detected collinearity between parameters of the linear forms of equations 4, 4a, and 4b. Hence, these equations were rejected to be inadequate to fit the corresponding data. On the other hand, collinearity between the parameters for the linear forms of eq 3 was not detected.

On the basis of the above results and by using eq 6 we calculated the k_1 and k_{-1} rate constants. In view of these estimates, we found that $k_2 \gg k_{-1}$ for all three amide substrates, and thus K_S equals k_2/k_1 . Furthermore, we assumed that $K_S = k_2/k_1$ is also valid for the ester substrate, although this is only true for a limited number of ester substrates of papain (9), and hence the relation $k_{cat}/K_m = k_1$ (25) appears to be valid for all four substrates. The results of best fit of eq 6 to the corresponding data are shown in Table 2 and could be presented by shapes identical to these appearing in Figure 2. The mean values of $\phi^{T,k1}$ and $\phi^{G,k1}$ fractionation factors between the amide substrates are 0.39 and 0.16, respectively, very similar to ϕ^T and ϕ^G reported for proton inventories of k_{cat}/K_m (Table 1).

Proton Inventories of K_S . Equation 3a best fitted the data for K_S , calculated through the relation $K_m = k_3 K_S/(k_2 + k_3)$ (9), as a function of deuterium atom fraction n ; the results are reported in Table 3 and in Figure 2. These PI exhibited high normal and essentially linear SIE; their linear character was validated by two methods. First, higher-order polynomials were fitted to the data; polynomials of the second or higher order were no longer justified statistically. Second, the parameter $DC = (K_S)_{0.5}/(K_S)_0 - [(K_S)_1/(K_S)_0 + 1]/2$

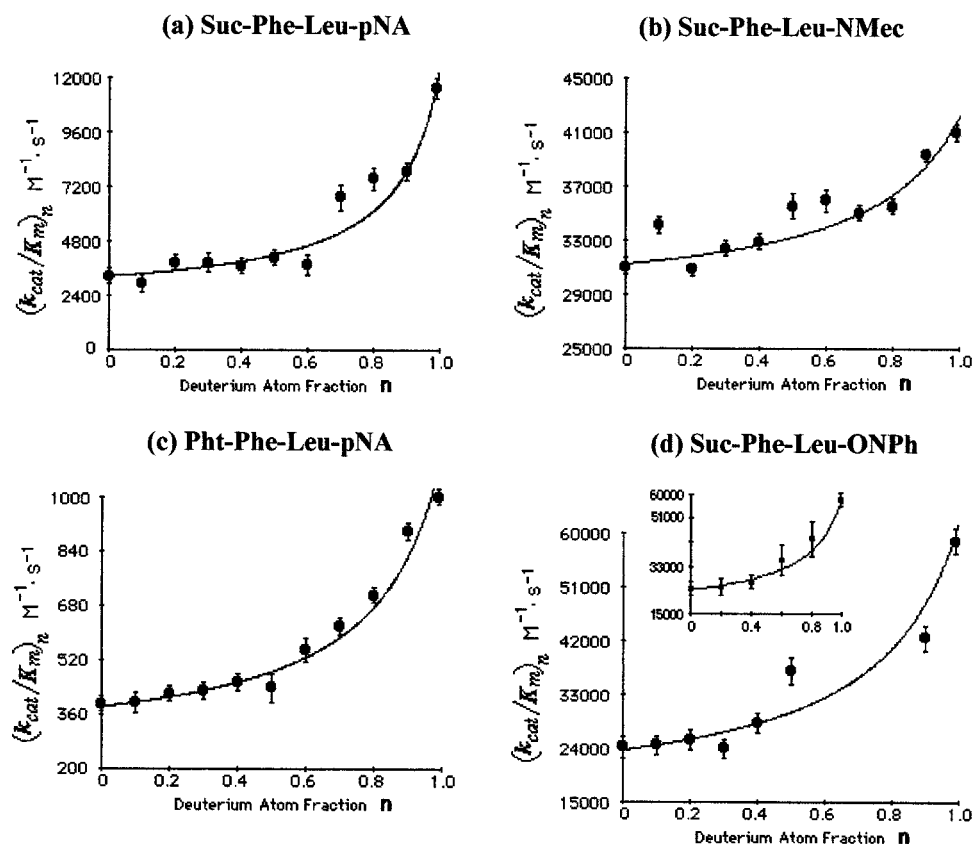


FIGURE 1: Nonlinear best fitting of eq 3 to the data for the k_{cat}/K_m parameter, for all four substrates. Solid lines were drawn according to all four requirements described in the analysis of data. All reactions were performed in 0.1 M phosphate buffer containing 1 mM K_2EDTA and 2 mM 1,4-dithiothreitol at pL 6.5. Complementary data from first-order progress curves were confirmed the best fit for the ester substrate (see inset to Figure 1, panel d).

Table 1: Parameter Estimates for Proton Inventories of k_{cat}/K_m ^a

substrate	$(k_{\text{cat}}/K_m)_0$ $\text{M}^{-1} \text{s}^{-1}$	ϕ^T	ϕ^G	SIE $1/D(k_{\text{cat}}/K_m)$
Suc-Phe-Leu-pNA	3200	0.45	0.12	3.8
Suc-Phe-Leu-NMec	31000	0.30	0.22	1.4
Pht-Phe-Leu-pNA	400	0.48	0.16	3.0
Suc-Phe-Leu-ONPh	24000	0.46	0.19	2.6

^a Equation 3 best fitted the experimental data for all four substrates by nonlinear least squares regression analysis. Mean values of 0.42 and 0.17 are calculated for the fractionation factors ϕ^T and ϕ^G , respectively, while the mean value of the inverse SIE is found 2.7. The standard deviations of all tabulated parameters were found lower than 1%; they are not given here to avoid overcrowding.

Table 2: Best-Fit Parameters (\pm Standard Deviations) Estimated Using Eq 6, for the Hydrolysis of the Amide Substrates Obtained by Nonlinear Least Square Regression Analysis^a

substrate	$(k_1)_0$ $\text{M}^{-1} \text{s}^{-1}$	$(k_{-1})_0 \text{s}^{-1}$	ϕ^{T,k_1}	ϕ^{G,k_1}
Suc-Phe-Leu-pNA	3500	0.09	0.33 ± 0.09	0.08 ± 0.04
Suc-Phe-Leu-NMec	34000	0.07	0.31 ± 0.01	0.23 ± 0.01
Pht-Phe-Leu-pNA	400	0.01	0.52 ± 0.03	0.17 ± 0.02

^a Mean values of 0.39 and 0.16 are calculated for the fractionation factors ϕ^P and ϕ^G , respectively. Standard deviations of the estimates of $(k_1)_0$ and $(k_{-1})_0$ are not calculated.

introduced earlier (30) was used, and values of $\ln(\text{DC} + 1)$ close to zero were calculated for all the amide substrates. Nonsignificant deviations from linearity were observed and can be easily explained (2). The mean values, for the fractionation factors ϕ^P and ϕ^G , were found to be 0.20 and

0.83, respectively, while the mean value of the SIE is found close to 5.

Proton Inventories of k_2 . Equation 3 best fitted all data for the k_2 parameter, as a function of deuterium atom fraction n , and the results are reported in Table 4 and in Figure 3. The mean values of the fractionation factors ϕ^T and ϕ^G , which are very similar for all amide substrates, were calculated as 0.48 and 0.90, respectively. The PI of $(k_2)_n$ were found to be essentially linear, being checked as in the case of $(K_S)_n$. Their $\ln(\text{DC} + 1)$ values were found close to zero, including nonsignificant deviations from linearity, explained also as above.

Proton Inventories of k_{cat} and/or k_3 . Although for all three amide substrates $k_{\text{cat}} = k_2 k_3 / (k_2 + k_3)$ comprises both acylation and deacylation of enzyme, for the ester substrate $k_{\text{cat}} \approx k_3$. We estimated the proton inventories for $(k_{\text{cat}})_n$ of Suc-Phe-Leu-ONPh and for $(k_3)_n$ of Pht-Phe-Leu-pNA. Equation 3 best fitted all corresponding data as a function of deuterium atom fraction n , and the results are reported in Table 5 and in Figure 5. The mean values of the fractionation factors ϕ^T and ϕ^G , which are very similar for the two substrates, were calculated as 0.44 and 1.08, respectively. In both cases, the PI were found essentially linear, their linearity being checked as in the case of $(K_S)_n$, and their $\ln(\text{DC} + 1)$ values were found close to zero.

DISCUSSION

The application of the proton inventory method to the hydrolysis of four newly synthesized substrates by papain

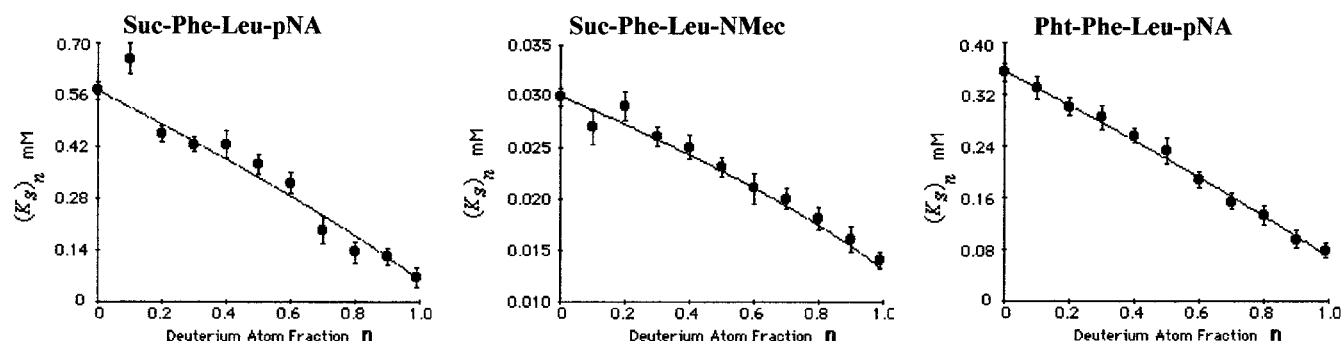


FIGURE 2: Nonlinear curve fitting of eq 3a to the data for $(K_S)_n$ of all amide substrates. All data are calculated as described in the text (see "analysis of data").

Table 3: Best-Fit Parameters (\pm Standard Deviations) Estimated Using Eq 3, for the Hydrolysis of the Amide Substrates Obtained by Nonlinear Least-Squares Regression Analysis^a

substrate	$(K_S)_0$ mM	ϕ^P	ϕ^G	SIE $D(K_S)$
Suc-Phe-Leu-pNA	0.57 ± 0.06	0.09 ± 0.03	0.87 ± 0.14	9.5
Suc-Phe-Leu-NMec	$0.03 \pm 6.5 \times 10^{-4}$	0.34 ± 0.07	0.73 ± 0.05	3.0
Pht-Phe-Leu-pNA	0.36 ± 0.01	0.16 ± 0.02	0.88 ± 0.04	5.15

^a Mean values of 0.20 and 0.83 are calculated for the fractionation factors ϕ^P and ϕ^G , respectively, while the mean value of the SIE is found 5.9.

Table 4: Parameter Estimates (\pm Standard Deviations) for Proton Inventories of k_2^a

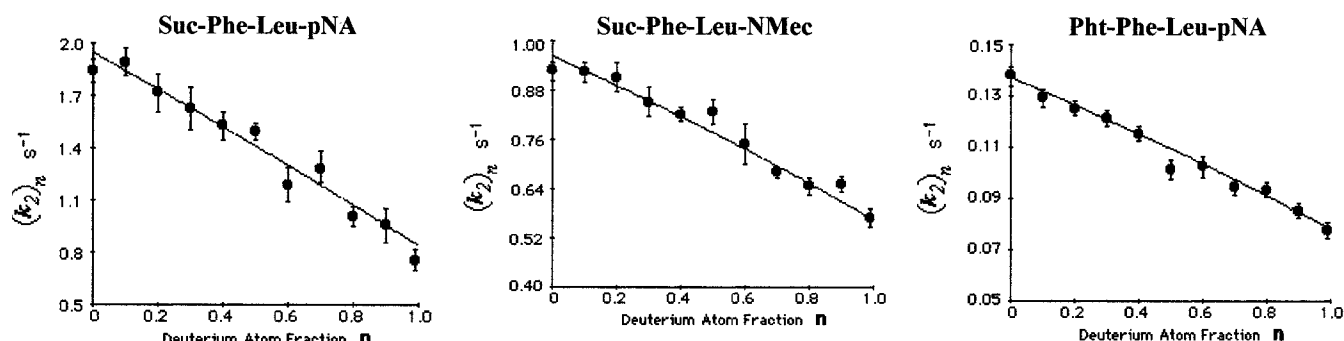
substrate	$(k_2)_0$ s ⁻¹	ϕ^T	ϕ^G	SIE $D(k_2)$
Suc-Phe-Leu-pNA	1.93 ± 0.06	0.41 ± 0.03	0.94 ± 0.06	2.3
Suc-Phe-Leu-NMec	0.96 ± 0.02	0.51 ± 0.03	0.87 ± 0.05	1.9
Pht-Phe-Leu-pNA	$0.14 \pm 2.0 \times 10^{-3}$	0.51 ± 0.02	0.89 ± 0.03	1.8

^a Equation 3 best fitted the experimental data for the amide substrates by nonlinear least square regression analysis. Mean values of 0.48 and 0.90 are calculated for the fractionation factors ϕ^T and ϕ^G , respectively, while the mean value of the SIE is 2.0.

led us to discover a new relationship between k_{cat} , K_m , and k_1 , namely, $k_{cat}/K_m = k_1$. The parameter K_S , which was found essentially equal to the ratio k_2/k_1 , and the rate constants k_1 , k_{-1} , and k_2 were calculated for all amide substrates. The interpretation of PI having similar shapes as those for k_{cat}/K_m has been based on the amount of curvature expressed by the gamma (γ) method of Alberty (31); when our PI for all four substrates were plotted as $\ln[(k_{cat}/K_m)_n]$ versus n , they exhibited greater-than-exponential curvatures and hence correspond to negative γ values (31). Such plots cannot be accounted for by an isotope effect arising from solvent reorganization. Moreover, they require the presence of discrete nonunit fractionation factors in the ground state (26). Our results from both original and alternative fitting are in agreement to previous interpretations of PI having similar shapes (26, 31). Therefore, the experimental data of the PI for k_{cat}/K_m , for all four substrates, are best analyzed by the nonlinear eq 3. Moreover, all parameter values reported in Table 1, as well as in Figure 1, describe unambiguously the

dependence of k_{cat}/K_m as a function of n for all four substrates. Thus, in all cases, for the reaction governed by k_{cat}/K_m (or k_1) the inverse isotope effect originates from two contributing exchangeable hydrogenic sites, one in the ground state and another in the transition state. The effective ground state of this reaction is free substrate, and free enzyme whose reactive thiolate-imidazolium ion-pair is likely to be in equilibrium with its tautomer neutral thiol-imidazole form (4–6). Alternatively, if there is not net charge localization between the side chains of active site Cys-25 and His-159 due to some relatively hydrophobic microenvironment, a low-barrier hydrogen bond (LBHB) may exist between them (12, 32). We considered that both LBHB and tautomerization equilibrium hypotheses are equally likely and display this effective ground state. Besides, both the pK_a of the protonated side chains of active site Cys-25 and His-159 are of similar magnitudes (33), and their covalent character becomes important because the two possible tautomeric forms of the ion-pair seems to be energetically equivalent because of their ionic character (34). Hence, a mean value of $\phi^G = 0.17$ could be assigned either to the tautomerization equilibrium through monomer or dimer water clusters (24; in Table 3) or to a low-barrier hydrogen bond formed as it is described above, as $\phi^G \approx 0.2$ (35).

Proton exchange takes place in ground states whose fractionation factors are directly measurable having characteristic values similar for the same functional groups (1, 2); however, transition states should be treated similarly due to ground-state equilibrium (2). Hence, we estimated a mean value of $\phi^T = 0.42$ for the PI of k_{cat}/K_m , which could be assigned to the ionization of the sulfhydryl group of active Cys-25 (ref 1; in Table 2, ref 24; in Table 3). Furthermore, the linear PI of both K_S and k_2 for all amide substrates exhibited relatively large normal SIE, which originate from one single site, in the product state and/or in the transition state, respectively. Since $K_S = k_2/k_1$ for all amide substrates, this parameter represents a dynamic equilibrium constant (36), and not a thermodynamic one as in cases where $K_S = k_{-1}/k_1$. Thus k_2 , which affects the K_S , strongly depends on the basicity of the nitrogen atom of the scissile amide bond, i.e., on the reason that promotes acylation; this basicity is decreased as n is increased and the reaction medium becomes less ionic. In addition, rounded-to-unit ϕ^G and small ϕ^T found for k_2 , indicate that the observed SIE in this rate constant is due to a hydrogen bridge in the transition state, for proton transfer (ref 24; in Table). Likewise, an interchange of a simple N-H bond in the tetrahedral complex to a LBHB in

FIGURE 3: Nonlinear curve fitting of eq 3 to the data for the $(k_2)_0$ parameter, for all amide substrates.Table 5: Parameter Estimates (\pm Standard Deviations) for Proton Inventories of k_3^a

substrate	$(k_3)_0$ s ⁻¹	ϕ^T	ϕ^G	SIE _{D(k₃)}
Pht-Phe-Leu-pNA	0.35 \pm 0.01	0.43 \pm 0.03	1.07 \pm 0.06	2.5
Suc-Phe-Leu-ONPh	7.85 \pm 0.02	0.45 \pm 0.01	1.09 \pm 0.02	2.4

^a Equation 3 best fitted the experimental data for the two substrates by nonlinear least square regression analysis. Mean values of 0.44 and 1.08 are calculated for the fractionation factors ϕ^T and ϕ^G , respectively, while the mean value of the SIE is 2.4.

the free enzyme occurs during acylation (37, 38). Therefore, a covalent intermediate on the reaction path to the acyl enzyme influences these K_S values (25, 39) as deuterium atom fraction n is increased, while a tetrahedral adduct is formed during the k_1 step (25, 40–42). These findings are in good agreement to the observed inverse SIE on the k_{cat}/K_m parameter, which seems more likely to be due to the disruption of the C–H⁺ ion-pair and the formation of a new interaction involving imidazolium cation and substrate (42). Accordingly, in the effective transition state of the reaction

governed by k_{cat}/K_m , a partial bond-making between the Cys-25 sulfur atom and the carbonyl carbon of the scissile bond occurs, while the double-bond character of the carbonyl carbon atom–carbonyl oxygen atom bond of the substrate, is partially reduced. Except for the relations $k_{cat}/K_m = k_1$ and $K_S = k_2/k_1$ found in this work, the last conclusion is supported also by previous ones suggested by others for serine proteases exhibiting $k_2/K_S = k_1$ (or $k_{cat}/K_m = k_1$) (25, 43, 44). Moreover, Angelides and Fink (45) have reported an irreversible reaction step observed before the formation of the acyl-enzyme during the hydrolysis of *N*^α-carbobenzoxy-L-lysine methyl ester by papain at subzero temperatures.

These results are novel and are reported here for the first time. Accordingly, Scheme 2 could describe, in agreement with our results, the binding of a substrate molecule, like those used herein for papain, as well as the acylation of papain by amide substrates, in good agreement to Scheme 2, where, A is free enzyme, B is the tetrahedral adduct, and C is the acyl-papain.

All four substrates used in this work have either the same acyl moiety (e.g., Suc-Phe-Leu-X) or the same leaving

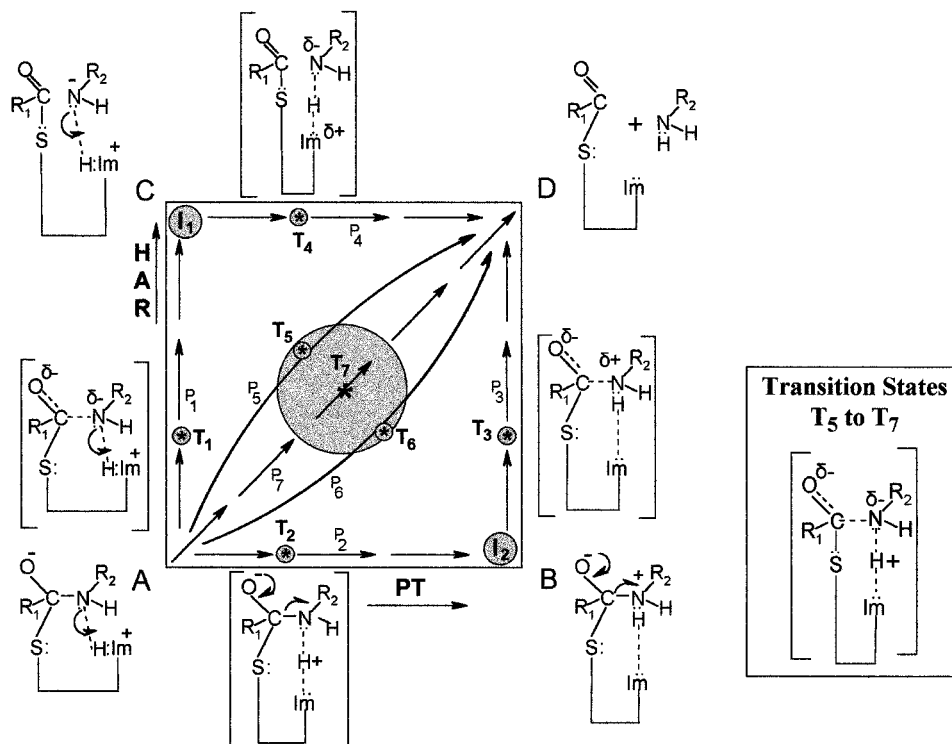


FIGURE 4: HAR/PT diagram: A is the reactant, and D is the product (acyl enzyme and free pNA), B or I₂ and C or I₁ are possible intermediates, T₁ to T₇ are possible transition states, and T₁ to T₄ correspond to stepwise pathways P₁ to P₄. The boxed diagram represents the most probable transition states T₅ to T₇, corresponding to the concerted pathways P₅ to P₇.

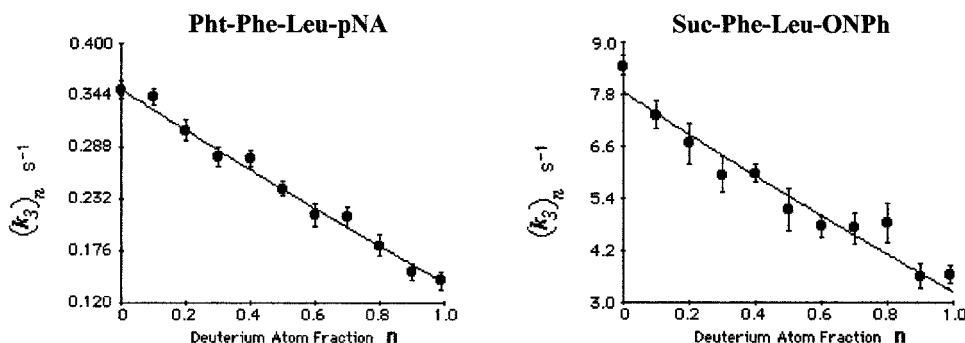
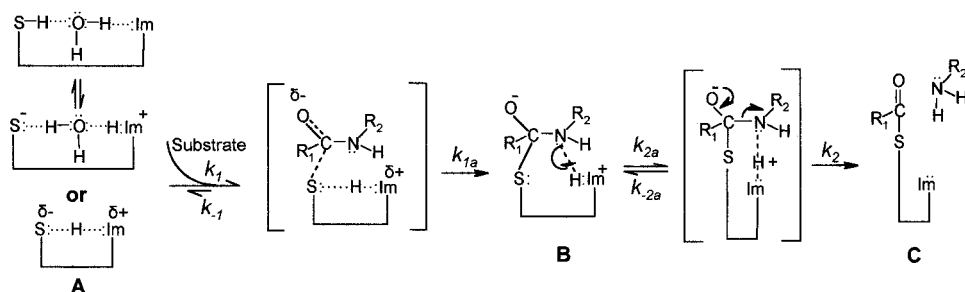
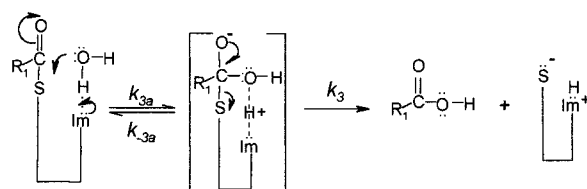


FIGURE 5: Nonlinear curve fitting of eq 3 to the data for the $(k_3)_0$ parameter for the substrates Pht-Phe-Leu-pNA and Suc-Phe-Leu-ONPh.

Scheme 2



Scheme 3



group (e.g., Suc-Phe-Leu-pNA, Pht-Phe-Leu-pNA). Thus, the detected linear character of PI of k_2 shows that papain acts as a one-proton catalyst during its acylation by the amide substrates whether they are acyl moieties and/or leaving groups. However, the calculated mean value of the fractionation factor $\phi^T = 0.48$ should be combined with more data to identify the species between which proton transfer is taking place. It has been shown that acylation of papain with amide substrates is facilitated by a hydrogen bond formation between the nitrogen atom of the scissile amide bond and the enzyme (4). Recent work reports on structural features of amide hydrolysis by papain based either on experimental work or on theoretical calculations. Other authors have shown that the attack of thiolate anion of the active site ion-pair C^-H^+ on the carbonyl carbon of scissile amide bond is a concerted rather than a stepwise proton transfer (10, 12, 40, 41).

Taking into account the above and other conclusions, together with our results from Table 4, we could construct a HAR/PT (heavy atom reorganization/proton transfer) diagram (Figure 4) for all amide nitroanilide substrates (2). The pK_a of free pNA is 1.0 (46); hence, we should assume a similar value for the pK_a of the nitrogen atom of tetrahedral adduct A in Figure 4 (43), while a $pK_a = 6.95$ is referred to for the imidazolium cation (44). On the other hand, the pK_a of the intermediate C in Figure 4 should meet that of an oxonium cation -1.74 , since it is actually the salt of an acid and a base, both of them being stronger than water, and thus

a HAR $\approx (6.95 - 1)/(6.95 + 1.74) = 0.68$ (2). Proton transfer (PT) should have an approximate value of 0.5 as $0.3 < \phi^T = 0.48 < 0.7$ (2). Accordingly, one proton is transferred spontaneously from the imidazolium cation onto the nitrogen atom, while the scissile amide bond is breaking off simultaneously to the formation of the acyl enzyme. In other words, acylation of papain proceeds via a concerted pathway through a transition state whose most probable form is that depicted in Figure 4 (2, 10, 12). This finding that is also novel supports the previously described mechanism in Scheme 2 in that it provides additional evidence that basicity of the nitrogen atom of the scissile amide bond is the reason, which promotes acylation (intermediate C in Figure 4). By making reasonable assumptions one could assign a $pK_a \approx 2$ to 7-amino-4-methylcoumarine, in analogy to that of pNA (46), and therefore we could construct an equivalent HAR/PT diagram for the amide NMec substrate with HAR ≈ 0.57 . Figure 4 is in full agreement to other results reported earlier (47), for reactions that involve proton transfer to or from atoms such as O, N, or S.

Finally, the linear character of the proton inventories of k_3 show that papain acts as a one proton catalyst during deacylation whatever the leaving group of the substrates; one exchangeable hydrogenic site in the transition state generates a normal SIE. The calculated mean value of $\phi^T = 0.44$ could easily be ascribed to the transfer of one proton from water, the nucleophile, to neutral Im of the active site His-15, in the transition state. This result agrees with previously

reported ones obtained with ester substrates (2) and can be interpreted in a similar way. The attack of the nucleophilic water molecule, the solvent, onto the carbonyl carbon of acyl-papain is a concerted rather than a stepwise proton transfer from this water molecule to the neutral imidazole group of the active site His-159. Thus, Scheme 3 can describe the deacylation of acyl-papain.

ACKNOWLEDGMENT

Authors would like to thank the unknown referees of *Biochemistry* for their valuable comments and constructive suggestions.

APPENDIX 1

Equation 20 of ref 19 is $[P_1] = At + B(1 - e^{-bt})$, where $A = k_{cat}[E]_0[S]_0/[S]_0 + K_m$ (apparent), $b = k_3 + \{k_2/(1 + (K_S/[S]_0))\}$, and $B = [E]_0\{k_2/(k_2 + k_3)\}^2/[1 + (K_m$ (apparent)/ $[S]_0\})^2$ (eq 24 of ref 21).

By the definition of k_{cat} , we can write that $k_2/(k_2 + k_3) = (k_2k_3)/[(k_2 + k_3)k_3] = k_{cat}/k_3$, and thus $B = (k_{cat}^2[E]_0/k_3^2)/[(1 + K_m/[S]_0)^2]$; we considered, here, that K_m (apparent) = K_m (estimated).

APPENDIX 2

$$(K_S)_n = \frac{(k_{-1})_n + (k_2)_n}{(k_1)_n} = \frac{(k_{-1})_0 \frac{1 - n + n\phi_1^{T,k-1}}{1 - n + n\phi_1^{G,k-1}} + (k_2)_0 \frac{1 - n + n\phi^{T,k2}}{1 - n + n\phi^{G,k2}}}{(k_1)_0 \frac{1 - n + n\phi^{T,k1}}{1 - n + n\phi^{G,k1}}}$$

We considered that $\phi^{T,k1} \equiv \phi^{T,k-1}$ and $\phi^{G,k2} \equiv \phi^{G,k-1}$, though by definition the ground state is the same for both k_{-1} and k_2 . Thus, from the previous relation and by taking into account the definition of K_S , which could be generally transformed to $k_{cat}/K_m = k_2/K_S$, we obtain the following:

$$(K_S)_n = \frac{(k_2)_n}{(k_{cat}/K_m)_n} = \frac{(k_{-1})_0}{(k_1)_0} \frac{(1 - n + n\phi^{G,k1})}{(1 - n + n\phi^{G,k2})} + \frac{(k_2)_0}{(k_1)_0} \frac{(1 - n + n\phi^{T,k2})}{(1 - n + n\phi^{T,k1})} = \frac{1 - n + n\phi^{G,k1}}{1 - n + nC_1} \left[\frac{k_{-1}}{k_1} + \frac{k_2}{k_1} \frac{1 - n + nC_2}{1 - n + n\phi^{T,k1}} \right] = \frac{1 - n + n\phi^{G,k1}}{1 - n + nC_1} \left[\frac{k_1 K_S - k_2}{k_1} + \frac{k_2}{k_1} \frac{1 - n + nC_2}{1 - n + n\phi^{T,k1}} \right]$$

If $K_R = k_2/k_1$ then

$$\frac{(k_2)_n}{(k_{cat}/K_m)_n} = \frac{(1 - n + n\phi^{G,k1})}{(1 - n + nC_1)} \left\{ \frac{k_2}{(k_{cat}/K_m)} + K_R \left[\frac{1 - n + nC_2}{1 - n + n\phi^{T,k1}} - 1 \right] \right\}$$

REFERENCES

- Schowen, K. B., and Schowen, R. L. (1982) *Methods Enzymol.* 87, 551–606.

- Szawelski, R. J., and Wharton, C. W. (1981) *Biochem. J.* 199, 681–692.
- Harmony, J. A. K., Himes, R. H., and Schowen, R. L. (1975) *Biochemistry* 14, 5379–5386.
- Polgár, L. (1979) *Eur. J. Biochem.* 98, 369–374, and cited references of Polgár, L.
- Wandinger, A., and Creighton, D. J. (1980) *FEBS Lett.* 116, 116–122, and cited references of Creighton, D. J.
- Ménard, R., Plouffe, C., Laflamme, P., Vernet, T., Tessier, D. C., Thomas, D. Y., and Storer, A. C. (1995) *Biochemistry* 34, 464–471, and cited references of Ménard, R.
- Baker, E. N., and Drenth, J. (1987) in *Biological Macromolecules and Assemblies Vol. 3 – Active Sites of Enzymes* (Jurnak, F. A., and McPherson A., Eds.) pp 314–367, John Wiley & Sons, New York.
- Brocklehurst, K., Willenbrock, F., and Salih E. (1987) in *Hydrolytic Enzymes* (Neuberger, A., and Brocklehurst K., Eds.) pp 39–158, Elsevier, Amsterdam.
- Bender, M. L., and Brubacher, L. J. (1966) *J. Am. Chem. Soc.* 88, 5880–5889.
- Arad, D., Langridge, R., and Kollman, D. A. (1990) *J. Am. Chem. Soc.* 112, 492–502.
- Ménard, R., and Storer, A. C. (1995) *Biol. Chem. Hoppe-Seyler* 373, 393–400.
- Harrison, M. J., Burton, N. A., and Hillier, I. H. (1997) *J. Am. Chem. Soc.* 119, 12285–12292.
- Blumberg, S., Schechter, I., and Berger, A. (1970) *Eur. J. Biochem.* 15, 97–102.
- Barrett, A. J., Kembhavi, A. A., Brown, M. A., Kirschke, H., Knight, C. G., Tamai, M., and Hanada K. (1982) *Biochem. J.* 201, 189–198.
- Bieth, J. G., Spiess, B., and Wermuth, C. G. (1974) *Biochem. Res.* 11, 350–357.
- Oyamada, H., Saito, T., Inaba, S., and Ueki, M. (1991) *Bull. Chem. Soc. Jpn.* 64, 1422–1424.
- Anderson, G. W., Zimmerman, J. E., and Callahan, F. M. (1966) *J. Am. Chem. Soc.* 88, 1338–1339.
- Tchoupé, J. R., Moreau, T., Gautier, F., and Bieth, J. G. (1991) *Biochim. Biophys. Acta* 1076, 149–151.
- Bender, M. L., Kézdy, F. J., and Wedler, F. C. (1967) *J. Chem. Educ.* 44, 84–88.
- BIOSOFT (1991) *UltraFit*, The Non-Linear Curve-fitting Package 5–58, Cambridge, U.K.
- Mannervik, B. (1982) *Methods Enzymol.* 87, 370–390.
- Cornish-Bowden A. (1995) in *Analysis of Enzyme Kinetic Data*, pp 11–16, Oxford Science Publications, New York, and cited references of Cornish-Bowden.
- Akaike, H. (1976) *Math. Sci.* 14, 5–9.
- Venkatasubban, K. S., and Schowen, R. L. (1985) *CRC Crit. Rev. Biochem.* 17, 1–44.
- Hirohara, H., Philipp, M., and Bender, M. L. (1977) *Biochemistry* 16, 1573–1580.
- Quigley, K., Szawelski, R. J., and Wharton, C. W. (1986) *Biochem. Soc. Trans.* 14, 167–181.
- Stein, R. L., Strimpler, A. M., Hori, H., and Powers J. C. (1987) *Biochemistry* 26, 1305–1314, and cited references of Stein, R. L.
- Ratkowsky, D. A., (1983) in *Nonlinear Regression Modeling, A Unified Practical Approach*, pp iii–v, Marcel Dekker Inc, New York.
- Chatterjee, S., and Price B. (1977) in *Regression Analysis by Example*, pp 9–18, John Wiley and Sons, New York.
- Matta, M. S., and Toenjes, A. A. (1985) *J. Am. Chem. Soc.* 107, 7591–7596.
- Albery, W. J. (1975) in *Proton-Transfer Reactions – Solvent Isotope Effects* (Caldin E., and Gold V., Eds.) pp 263–315, Chapman & Hall, London.
- Golubev, N. S., Shenderovich, I. G., Smirnov, S. N., Denisov, G. S., and Limbach, H.-H. (1999) *Chem. Eur. J.* 5, 492–497.
- Ménard, R., Khouri, H. E., Plouffe, C., Laflamme, P., Dupras, R., Vernet, T., Tessier, D. C., Thomas, D. Y., and Storer, A. C. (1991) *Biochemistry* 30, 5531–5538.

34. Perrin, C. L., and Nielson, J. N. (1997) *Annu. Rev. Phys. Chem.* 48, 511–544.
35. Kreevoy, M. M., Liang, T.-m., and Chang, K.-C. (1979) *J. Am. Chem. Soc.* 76, 557–560.
36. Dixon, M., and Webb E. C. (1971) in *Enzymes*, 2nd ed., pp 92–111, Longman, London.
37. Eliason R., and Kreevoy, M. M. (1978) *J. Am. Chem. Soc.* 100, 7037–7041.
38. Gerlt J. A., and Gassman, P. G. (1993) *Biochemistry* 32, 11943–11952.
39. Zeeberg, B., Caplow, M., and Caswell, M. (1975) *J. Am. Chem. Soc.* 97, 7346–7352.
40. Fersht, A. R. (1971) *J. Am. Chem. Soc.* 94, 3504–3515.
41. Frankfater A., and Kuppy, T. (1981) *Biochemistry* 20, 5517–5524.
42. Brocklehurst, K., Kowlessur, D., Patel, G., Templeton, W., Quigley, K., Thomas, E. W., Wharton, C. W., Willenbrock, F., and Szawelski, R. J. (1988) *Biochem. J.* 250, 761–772.
43. Komiyama, M., and Bender, M. L. (1979) *Proc. Natl. Acad. Sci. U.S.A.* 99, 5207–5209.
44. Fersht, A. (1977) in *Enzyme Structure and Mechanism*, pp 103–154, W. H. Freeman and Co Ltd., San Francisco.
45. Angelides, K. J., and Fink, A. L. (1978) *Biochemistry* 13, 2659–2668.
46. Morrison, R. T., and Boyd R. N. (1992) in *Organic Chemistry*, 6th ed., pp 713–751 and pp 821–883, Prentice Hall, New Jersey.
47. Jencks, W. P. (1972) *Chem. Rev.* 72, 705–718.

BI001615B